Supporting Information

Bozkurt et al. 10.1073/pnas.0910223106

SI Materials and Methods

Cloning, Expression, and Purification. The constructs of *C. therm. get3* encoding amino acids 1–339 ($Get3_{FL}$) and 14–339 (Get3) were amplified from a cDNA bank provided by S.A. and E.H. Cloning into pET24d by PCR using the PciI and BamHI restriction sites resulted in a C-terminal hexa-histidine tag. Constructs of *get3*/*ramp4* (*C. therm.*/*C. therm.*) and *get3*/*ramp4op* (*C. therm.*/*Mus musculus*) were cloned into the polycistronic vector pst39 (1) using XbaI/BamHI for Get3 and EcoRI/Hin*d*III for Ramp4 or Ramp4op restriction sites, leading to an N-terminal hexa-histidine tag and a C-terminal opsin tag in Ramp4op. All DNA constructs were sequenced by AGOWA, Berlin.

$Get3_{FL}$ and Get3 were overexpressed in the *E. coli* BL21(DE3) Rosetta strain (Novagen) at 30 °C in the presence of 1.5% (wt/vol) D^+-lactose. After overnight induction, cells were harvested and stored at −80 °C. Cell pellets were resuspended in buffer A [10 mM Tris-Cl, 500 mM NaCl, 20 mM imidazol, 1 mM $MgCl_2$, 5% (vol/vol) glycerol, pH 8.0]. Cells were lysed using a Microfluidizer M1–10L (Microfluidics), and the lysate was cleared by ultracentrifugation at 91,000 × *g* for 40 min at 4 °C. The supernatant was applied to a 1-mL His-Trap HP column (GE Healthcare). The column was washed with 10 column volumes of buffer A and buffer A containing 50 mM imidazol. Bound Get3 was eluted with buffer A supplemented with 300 mM imidazol. Get3 was further purified by SEC (Superdex 200 26/60; GE Healthcare) in a buffer containing 10 mM Tris-Cl (pH 8.0), 150 mM NaCl, and 1 mM $MgCl_2$. Basically, a similar protocol was used for the Get3–Ramp4 and Get3–Ramp4op complexes.

Crystallization and Data Collection. Crystals of *C. therm.* Get3 were grown at 4 °C by the sitting drop vapor diffusion method. Sitting drops were prepared by mixing 1 μL of fresh Get3 protein (10 mg/mL) in the presence of 5 mM ADP or AMPPNP with 1 μL of reservoir solution containing 0.1 M Tris (pH 8.5), 50 mM $MgCl_2$, and 35% (vol/vol) ethanol. Crystals were flash-frozen directly or after the addition of 20% (vol/vol) ethylene glycol in liquid nitrogen. Data were collected at 100 K at beamlines ID23–1 and ID23–2 at the European Synchrotron Radiation Facility. Data were processed using IMOSFLM and SCALA (2) or XDS and XSCALE (3).

Structure Determination and Refinement. Both Get3 structures were solved by molecular replacement using the CCP4-implemented program PHASER (4). The AMPPNP-Mg^{2+}-bound structure was solved by using a single ATPase subdomain of ArsA (PDB ID code 1f48) as a search model. The ADP-Mg^{2+}-bound structure was solved with the AMPPNP-Mg^{2+}-bound structure. For refinement, we used the REFMAC5 program (5). Both structures were refined by TLS and NCS refinement in REFMAC5 after iterative model building in COOT (6). The model quality was analyzed with PROCHECK (7) and WHATIF (8). The multiple sequence alignment was performed with the JalView program (9). Disordered secondary structure elements in *C. therm.* Get3 were modeled according to the PsiPred secondary structure prediction server (10). Figures were generated by PyMOL (DeLano Scientific).

Atomic coordinates and structure factors for the AMPPNP-Mg^{2+}-bound and ADP-Mg^{2+}-bound crystal structures of *C. therm*. Get3 have been deposited in the Protein Data Bank with the accession codes 3IQW and 3IQX, respectively.

AUC. Oligomerization states of Get3 and the Get3–Ramp4 complex from *C. therm.* were analyzed in sedimentation velocity experiments using a Beckman Optima XL-A analytical ultracentrifuge equipped with absorbance optics and an An60 Ti rotor (Beckman Coulter, Fullerton, CA). Experiments were carried out at 35,000 rpm and 20 °C at protein concentrations of 50–100 μM Get3, corresponding to an absorbance of 0.5–1 at 280 nm. Partial specific volumes, extinction coefficients, and buffer density and viscosity were calculated with the SEDNTERP software program (http://www.rasmb.bbri.org/). For data analysis, the SEDFIT program was used to determine c(s) and c(M) distribution of sedimentation coefficients and molecular weight, respectively (11, 12). Theoretical hydrodynamic parameters were calculated with HYDROPRO (13) from the Get3 crystal structure, and for the Get3/Ramp4 tetramer, a head-to-head model was created composed of spherical beads 3.3 Å in size.

Amide HX-MS Experiments. Amide HX-MS experiments were performed similar to those described earlier (14, 15). Amide HX was initiated by a 20-fold dilution of either 200 pmol Get3 (apo), Get3 with an excess of nucleotides, or Get3–Ramp4 complex into D_2O buffer containing 20 mM Tris-Cl (pH 8.0), 150 mM NaCl, 15 mM $MgCl_2$, and 1 mM DTT at 30 °C. After various time intervals (10 s to 1 h), the exchange reaction was quenched by decreasing the temperature to 0 °C and the pH with ice-cold quench buffer (400 mM KH_2PO_4/H_3PO_4, pH 2.2). Quenched samples were then injected into an HPLC-MS setup as described. Only 2 M guanidium hydrochloride was omitted from the quenching buffer for the analysis of the peptide fragments. The deuteron content of the peptic peptides covering the $Get3_{FL}$ and the Get3–Ramp4 complex were determined from the centroid of the molecular ion isotope envelope. The deuteron content was calculated after adjustment for deuteron gain/loss during digestion and HPLC-MS setup. For this adjustment, nondeuterated and fully deuterated Get3 were analyzed (16). Fully deuterated samples were prepared by 3 cycles of drying and resolubilization in D_2O containing 6M guanidium hydrochloride. The 0% control was not treated with D_2O.

Membrane Insertion Assay. RMs were prepared as described by Walter and Blobel (17) and resuspended at an OD_{280} of 50 per milliliter in RM buffer [50 mM Hepes-KOH (pH 7.6), 50 mM KOAc, 2 mM $Mg(OAc)_2$, 250 mM sucrose, 2 mM DTT]. Trypsin-treated RMs (T-RMs) were obtained after incubation with 20 μg/mL Trypsin-Type XI (Sigma-Aldrich) for 1 h at 4 °C. The digestion was stopped by adding RM buffer complemented with 2 mM PMSF and 10 μg/mL aprotinin. T-RMs were then pelleted and resuspended in RM buffer. Purified *C. therm.* Get3-Ramp4op complex was incubated in a 10-μL reaction (200 nM final concentration) with 1 eq of RM, 1 mM ATP or other nucleotides, 1 mM $Mg(OAc)_2$, 40 mM Hepes (pH 7.6), and 80 mM KOAc. The insertion was carried out for 30 min at 30 °C and stopped by adding SDS/PAGE sample buffer. N-linked oligosaccharides were removed by EndoH treatment according to the manufacturer's instructions (New England Biolabs). Proteins were separated using a 16.5% (vol/vol) Schägger gel. Western blot analyses were performed with α-opsin antibodies (18–20). The amount of glycosylated Ramp4op observed with different nucleotides was quantified using ImageJ software (National Institutes of Health, http://rsb.info.nih.gov/ij/). Values were normalized to the amount of glycosylated Ramp4op detected in the presence of ATP.

1. Tan S (2001) A modular polycistronic expression system for overexpressing protein complexes in Escherichia coli. *Protein Expression Purif* 21:224–234.
2. Bailey S (1994) The CCP4 Suite—Programs for Protein Crystallography. *Acta Crystallogr D* 50:760–763.
3. Kabsch W (1993) Automatic processing of rotation diffraction data from crystals of initially unknown symmetry and cell constants. *J Appl Crystallogr* 26:795–800.
4. Read RJ (2001) Pushing the boundaries of molecular replacement with maximum likelihood. *Acta Crystallogr D* 57:1373–1382.
5. Murshudov GN, Vagin AA, Dodson EJ (1997) Refinement of macromolecular structures by the maximum-likelihood method. *Acta Crystallogr D* 53:240–255.
6. Emsley P, Cowtan K (2004) COOT: Model-building tools for molecular graphics. *Acta Crystallogr D* 60:2126–2132.
7. Laskowski RA, Macarthur MW, Moss DS, Thornton JM (1993) Procheck—A program to check the stereochemical quality of protein structures. *J Appl Crystallogr* 26:283–291.
8. Vriend G (1990) What if—A molecular modeling and drug design program. *J Mol Graphics* 8:52–56.
9. Waterhouse AM, Procter JB, Martin DM, Clamp M, Barton GJ (2009) Jalview version 2—A multiple sequence alignment editor and analysis workbench. *Bioinformatics* 25:1189–1191.
10. McGuffin LJ, Bryson K, Jones DT (2000) The PSIPRED protein structure prediction server. *Bioinformatics* 16:404–405.
11. Dam J, Schuck P (2004) Calculating sedimentation coefficient distributions by direct modeling of sedimentation velocity concentration profiles. *Methods Enzymol* 384:185–212.
12. Schuck P (2000) Size-distribution analysis of macromolecules by sedimentation velocity ultracentrifugation and lamm equation modeling. *Biophys J* 78:1606–1619.
13. Garcia De La Torre J, Huertas ML, Carrasco B (2000) Calculation of hydrodynamic properties of globular proteins from their atomic-level structure. *Biophys J* 78:719–730.
14. Rist W, Jorgensen TJ, Roepstorff P, Bukau B, Mayer MP (2003) Mapping temperature-induced conformational changes in the Escherichia coli heat shock transcription factor sigma 32 by amide hydrogen exchange. *J Biol Chem* 278:51415–51421.
15. Rist W, Graf C, Bukau B, Mayer MP (2006) Amide hydrogen exchange reveals conformational changes in hsp70 chaperones important for allosteric regulation. *J Biol Chem* 281:16493–16501.
16. Zhang Z, Post CB, Smith DL (1996) Amide hydrogen exchange determined by mass spectrometry: Application to rabbit muscle aldolase. *Biochemistry* 35:779–791.
17. Walter P, Blobel G (1983) Preparation of microsomal membranes for cotranslational protein translocation. *Methods Enzymol* 96:84–93.
18. Favaloro V, Spasic M, Schwappach B, Dobberstein B (2008) Distinct targeting pathways for the membrane insertion of tail-anchored (TA) proteins. *J Cell Sci* 121:1832–1840.
19. Scoulica E, Krause E, Meese K, Dobberstein B (1987) Disassembly and domain structure of the proteins in the signal-recognition particle. *Eur J Biochem* 163:519–528.
20. Adamus G, et al. (1991) Anti-rhodopsin monoclonal-antibodies of defined specificity—Characterization and application. *Vision Res* 31:17–31.

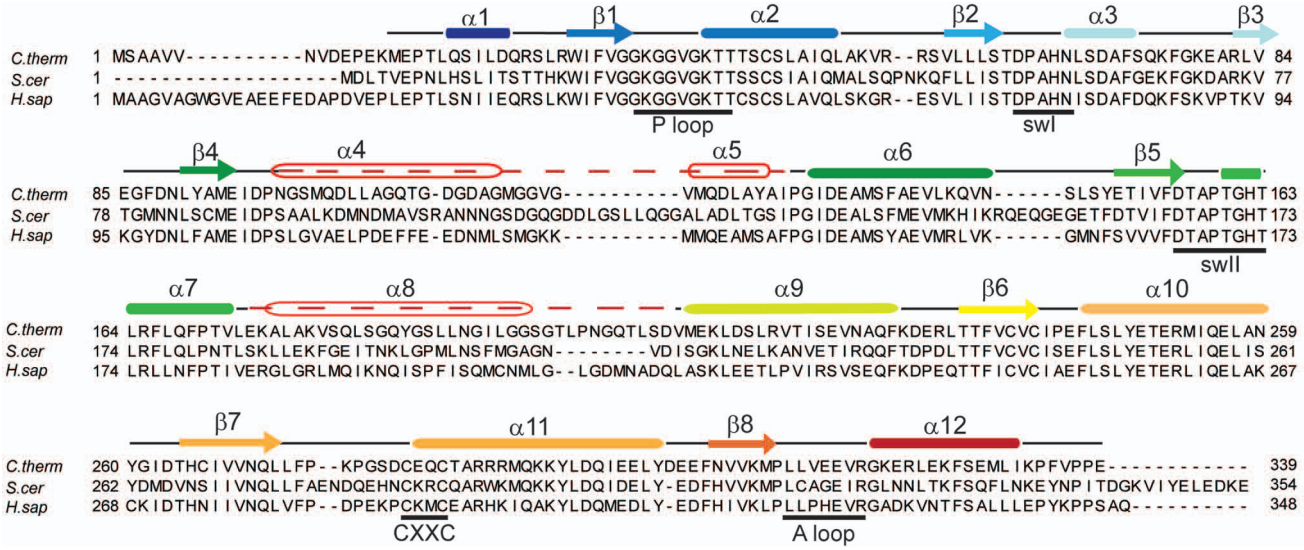

Fig. S1. Multiple sequence alignment of Get3 homologs. Sequences are from *C. therm.*, *S. cerevisiae*, and *H. sapiens*. The secondary structure derived from the crystal structure of *C. therm.* Get3 is shown above the sequences. Coloring of secondary structure elements is done in a ramp from blue (N-terminus) to red (C-terminus). Disordered regions in the crystal structure are indicated by a dashed red line. Important motifs such as the P-loop, switch I (swI), switch II (swII), Zn-interacting cysteines (CXXC), and A-loop are indicated with a black bar underneath the sequences.

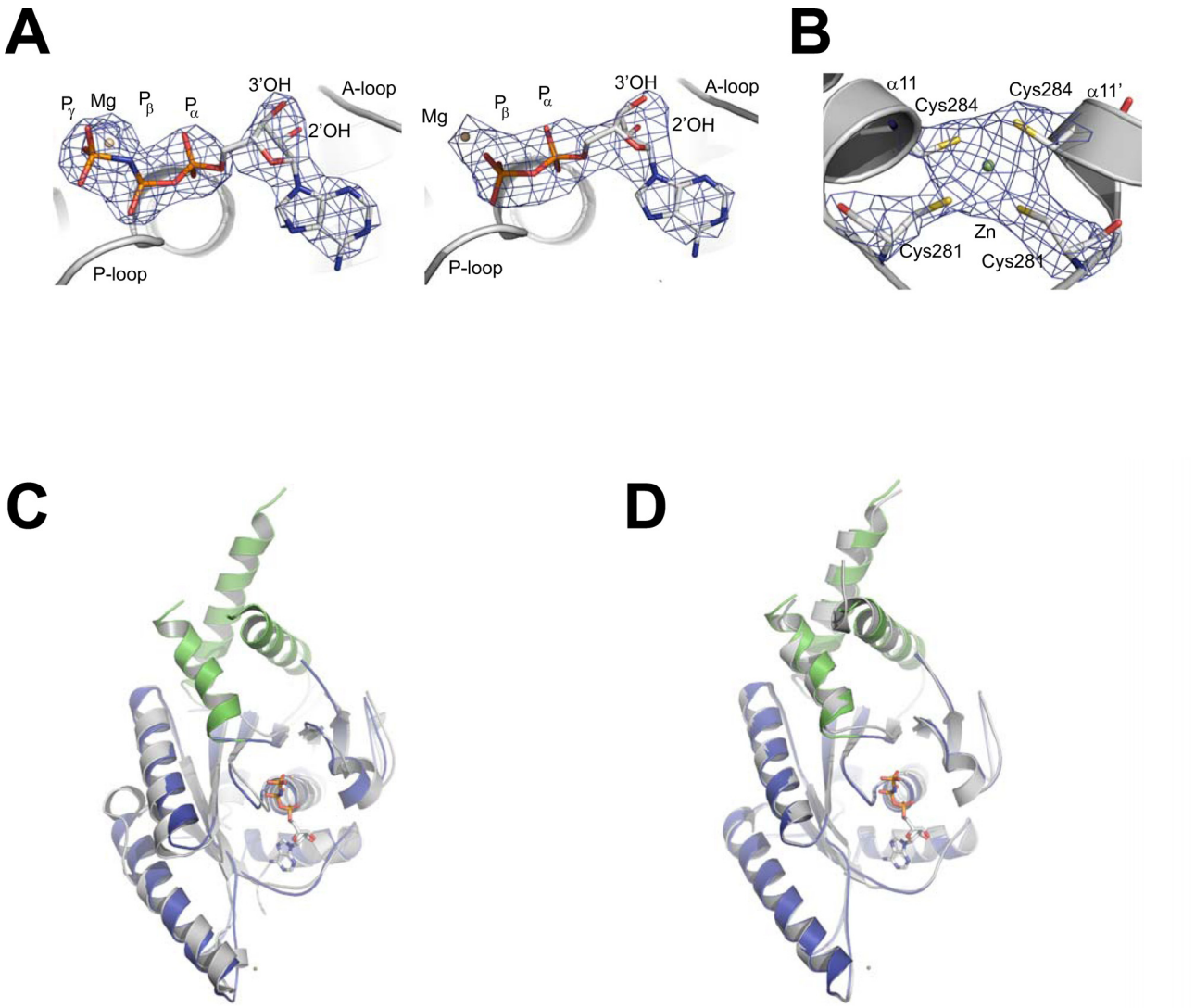

Fig. S2. Structural comparisons of *C. therm.* Get3. (*A*) Electron densities for *C. therm.* Get3 with bound AMPPNP-Mg^{2+} (*Left*) and ADP-Mg^{2+} (*Right*). The electron densities are shown for a σ_A-weighted $2mF_o$-DF_c map contoured at 2σ. (*B*) Details of the Zn^{2+}-binding site between 2 monomers of the AMPPNP-Mg^{2+}-bound Get3. The Zn^{2+} ion (green sphere) is coordinated by C281 and C284 from the conserved CXXC motif (Fig. 1*A*). The identity of the Zn^{2+} ion was determined by several independent methods. Induced coupled plasma MS indicated 1 Zn^{2+} ion per protein dimer (data not shown; M. Krachler, Heidelberg). An x-ray fluorescence spectrum of single crystals clearly showed a peak at the zinc absorption edge. Final evidence was provided after the structure was solved by the electron density and the tetrahedral geometry of the coordinating cysteine residues. The electron density is shown for a σ_A-weighted $2mF_o$-DF_c map contoured at 2σ. (*C*) Superposition of a monomer from the *C. therm.* Get3 AMPPNP-Mg^{2+}-bound structure (subdomains in green and blue) with the ATPase subdomain of ArsA (gray; PDB ID code 1f48). The structure of the ATPase subdomain of ArsA was used for molecular replacement to determine the structure of Get3 bound to AMPPNP-Mg^{2+}. The 2 domains superimpose with an rmsd of 1.58 Å over 169 residues. (*D*) Superposition of a monomer from the *C. therm.* Get3 AMPPNP-Mg^{2+}-bound structure (subdomains in green and blue, same coloring as in Fig. 1*C*) with the ADP-Mg^{2+}-bound structure (gray). The AMPPNP-Mg^{2+} structure was used as a search model to solve the structure of the ADP-Mg^{2+}-bound structure by molecular replacement (*SI Materials and Methods*). The 2 monomers superimpose with an rmsd of 0.5 Å over 259 residues.

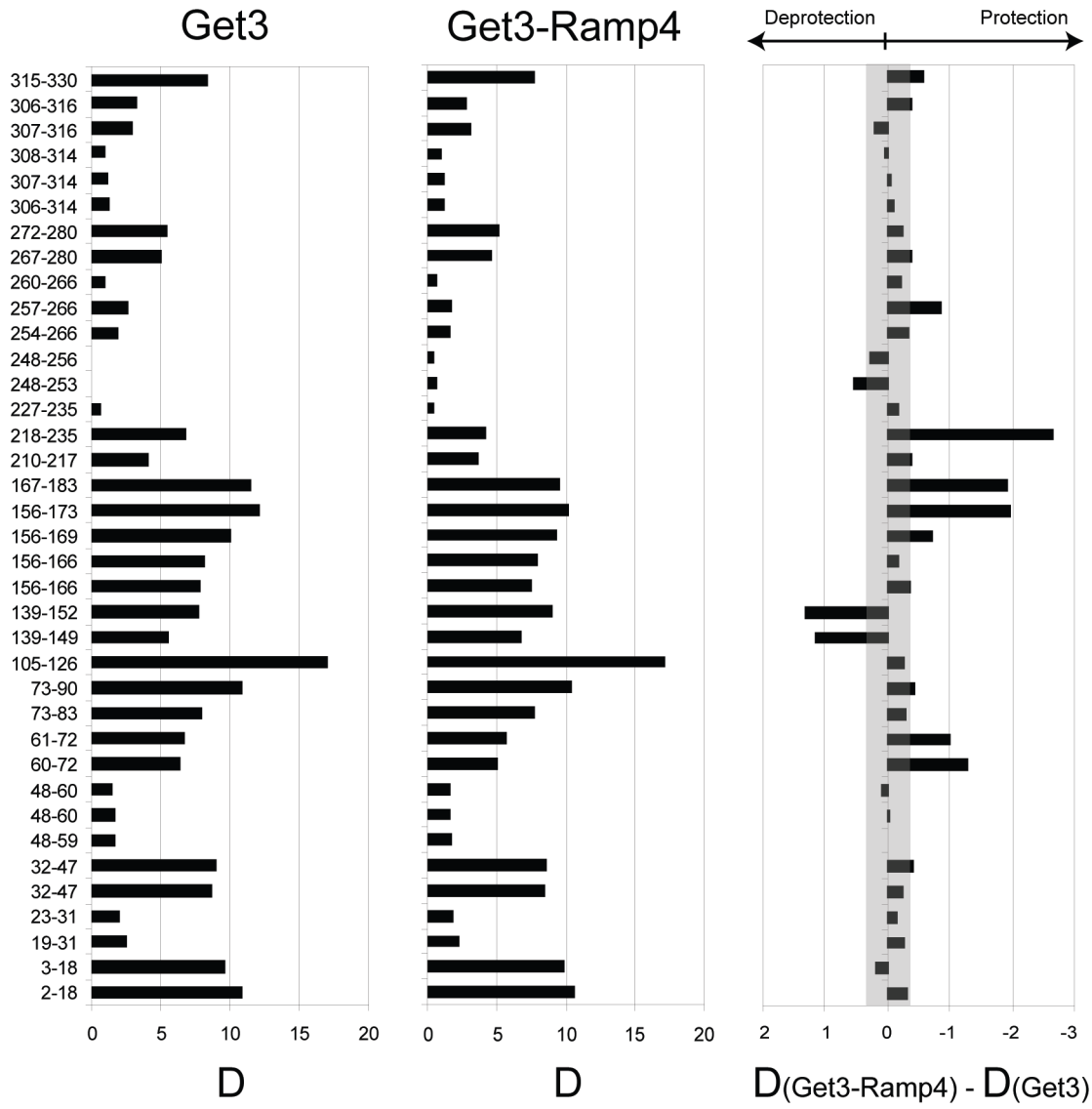

Fig. S3. HX-MS analysis of Get3 and the Get3–Ramp4 complex. Deuteron incorporation into Get3 in the absence of nucleotide and Ramp4 (*Left*) and into Get3 in the presence of Ramp4 (*Middle*) after 10 s of incubation in D_2O. (*Right*) Difference plot of deuteron incorporation in the Get3-Ramp4 complex minus Get3 alone. The numbers corresponding to the protein segments are indicated on the left. In the difference plot, bars to the right indicate Ramp4-induced protection (less deuteron incorporation) and bars to the left indicate a Ramp4-induced increase in solvent accessibility. (*Right*) Gray area gives the average SE.

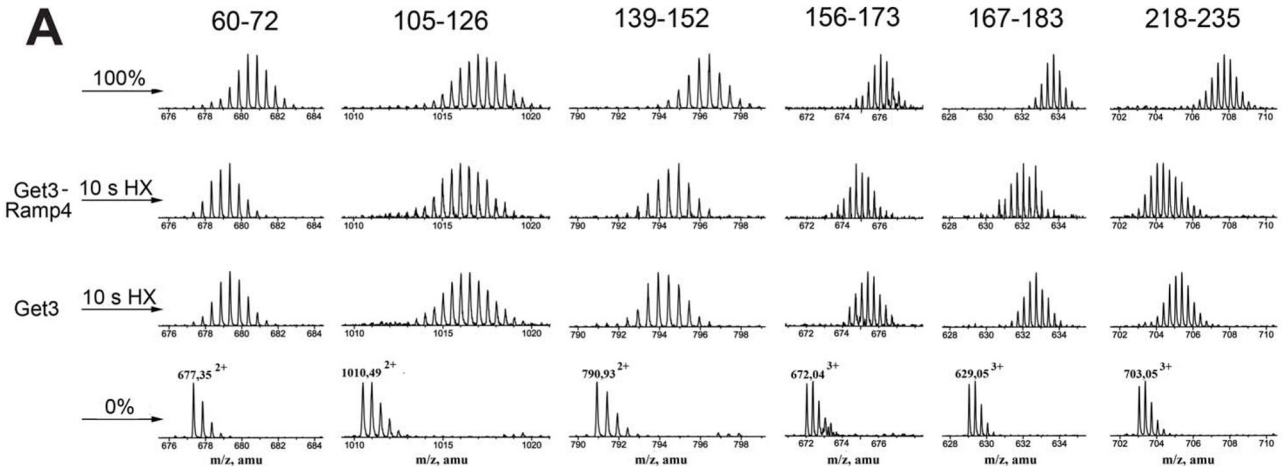

B

	Get3			Get3-Ramp4		
HDX Profile	Nr. Residues	k/min^{-1}	$t_{1/2}$ / min	Nr. Residues	k/min^{-1}	$t_{1/2}$ / min
Fast	205 ± 7	14.47 ± 2.21	0.05	192 ± 7	14.77 ± 2.26	0.05
Intermediate	57 ± 12	0.21 ± 0.09	3.3	61 ± 11	0.23 ± 0.09	3.04
Slow	67 ± 12	0.002 ± 0.0039	341.16	68 ± 11	0.0027 ± 0.0036	252.08

Fig. S4. Details of the HX-MS analysis of Get3 and the Get3–Ramp4 complex. (*A*) Effects of Ramp4 on deuteron incorporation into selected segments of Get3. Mass spectra of selected peptic peptides of Get3 in the absence and presence of Ramp4 after pulse labeling for 10 s in D_2O, as indicated on the left. The spectra of the peptic peptides in the undeuterated (*Bottom*, 0%) and the fully deuterated (*Top*, 100%) states are shown for comparison. The numbers above the spectra refer to the corresponding peptic peptides. The duration of labeling (10 s) was calculated to be sufficient to deuterate freely solvated amides selectively (1). (*B*) Exchange kinetics of Get3 and the Get3–Ramp4 complex. Observed rate constants are derived from a nonlinear triple-exponential regression fit of the deuterons incorporated over time. For this fit, the total amplitude was fixed to the Get3 total number of exchangeable amide hydrogens (329 for Get3 and 321 for Get3–Ramp4 complex). Global exchange data were adjusted for deuteron loss during analysis (2). The global exchange data do not show large differences between Get3 and the Get3–Ramp4 complex. This indicates either that Ramp4 binding does not induce large secondary structure changes or solvent exclusion. Alternatively, deprotected and protected regions could balance each other. The latter explanation was ruled out by a peptide analysis, as shown in Fig. S4*A*.

1. Bai Y, Milne JS, Mayne L, Englander SW (1993) Primary structure effects on peptide group hydrogen exchange. *Proteins* 17:75–86.
2. Zhang Z, Post CB, Smith DL (1996) Amide hydrogen exchange determined by mass spectrometry: Application to rabbit muscle aldolase. *Biochemistry* 35:779–791.

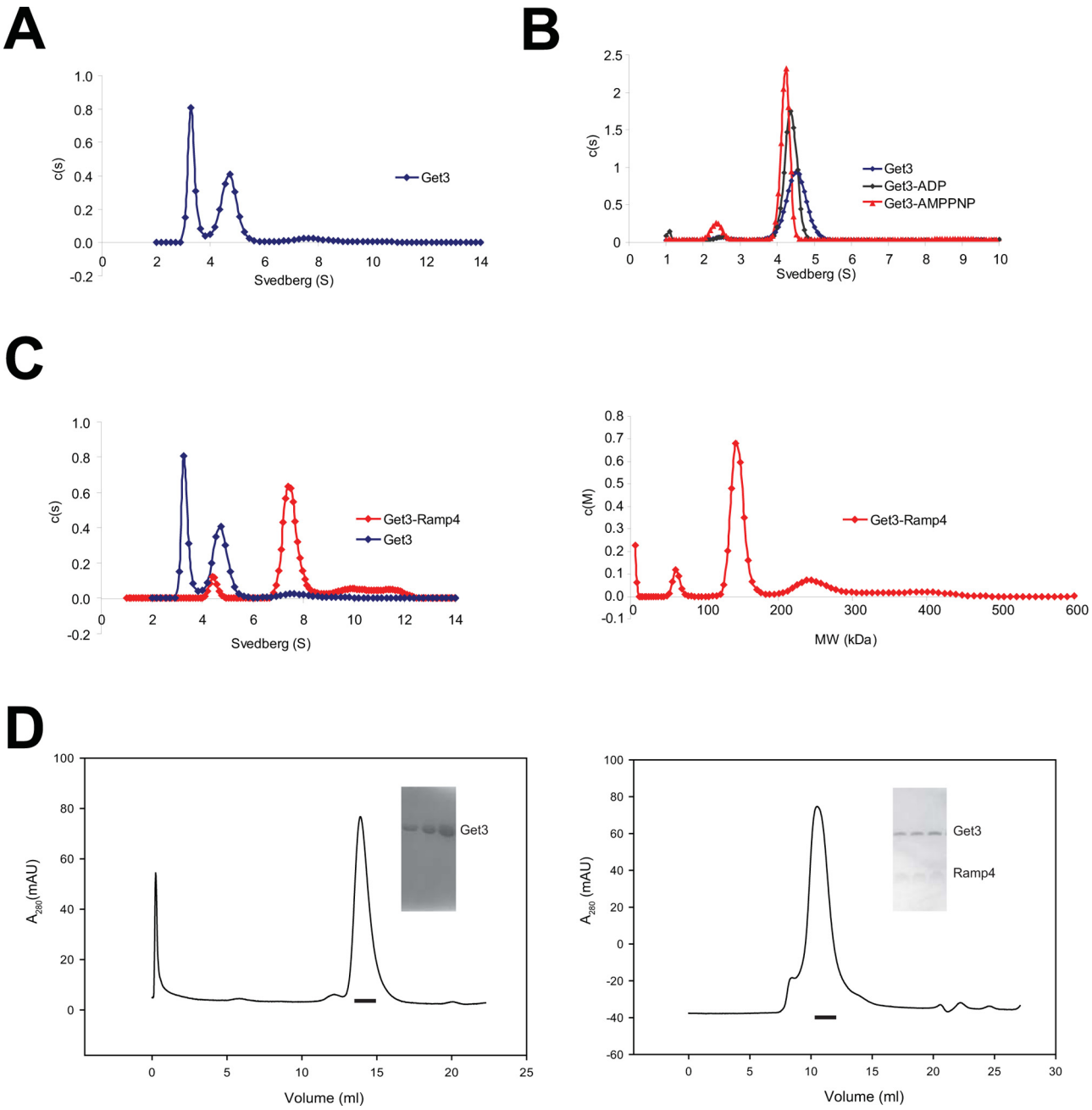

Fig. S5. Analysis of the oligomeric state of Get3 and the Get3–Ramp4 complex. (*A*) Oligomerization behavior of Get3 (blue) studied by AUC. For the sedimentation velocity runs, the distributions of sedimentation coefficients are shown. The monomer (3.09S), dimer (4.45S), and tetramer (7.73S) correspond to molecular masses of 37.5, 62.7, and 144.0 kDa, respectively. The s values were corrected for solvent density and viscosity of the buffer. (*B*) Oligomerization behavior of Get3 in the absence (blue) and presence of nucleotides: ADP (gray) and AMPPNP (red). For the sedimentation velocity runs, the distributions of sedimentation coefficients are shown. Nucleotide binding induces a slight shift to a lower sedimentation coefficient, indicating closure of the Get3 dimer. (*C*) Oligomerization behavior of the Get3–Ramp4 complex (red). Distributions of sedimentation coefficients (*Left*) and c(M) distribution (*Right*) are shown. The Get3–Ramp4 complex is mainly present as a higher oligomer with a sedimentation coefficient of 7.39S (corresponding to a molecular mass of 136 kDa), indicative of a tetramer. (*D*) Analysis of Get3 and Get3–Ramp4 complex by SEC. Get3 alone (*Left*) or a Get3-Ramp4 complex (*Right*) was subjected to SEC using a Superdex 200 (10/300) column. Peak fractions were collected (indicated by a black bar) and analyzed by SDS/PAGE (*Inset*).

Table S1. Data collection and refinement statistics

Get3 complex	AMMPNP-Mg^{2+}	ADP-Mg^{2+}
Data collection		
Wavelength, Å	0.8726	0.8726
Space group	$P2_12_12_1$	$P2_12_12_1$
Cell dimensions, Å		
a, b, c	46.57, 105.73, 136.93	46.75, 105.59, 137.35
Resolution range, Å	57.5–3.0 (3.16–3.0)	50–3.5 (3.7–3.5)
R_{sym}, %	7.8 (24.3)	24.6 (67.1)
$I/\sigma(I)$	13.9 (5.6)	6.6 (3.1)
Completeness, %	100 (100)	100 (100)
Redundancy	4.0 (4.1)	3.5 (3.4)
Unique reflections	14,221	9,088
B-factor, $Å^2$	42	52
Refinement		
Resolution, Å	52.9–3.0	49.3–3.5
No. reflections	13,509	8,633
R/R_{free}, %	22.8/27.1	22.9/29.5
No. atoms	4,187	4,178
Protein	4,117	4,121
Ligand/ions	70	57
Bond length, Å	0.018	0.019
Angle, °	1.84	2.03
Ramachandran plot quality, %		
Allowed region	87.6	84.2
Additionally allowed	12.4	15.6
Generously allowed	0	0.2

B-factor according to the Patterson function.
Values in parentheses are for the highest resolution shell.